# Coupled Thermomechanical Forging Simulations and the Effect of Material Constitutive Laws

Stuart Brown, Nagi Elabbasi, and Eric Schmitt

Veryst Engineering, LLC

***Abstract:*** *Correct hot forming design relies on accurate prediction of forming loads, material deformation, and material properties. This is particularly true for coupled thermomechanical analyses, where die/workpiece contact will change local deformations and temperatures. These strains and thermal histories can change the material microstructures and resulting product properties. This presentation examines the influence of different material and contact models within a hot forging simulation and discusses the consequences on ultimate product performance. We use rate-independent plasticity and compare the results with the Anand internal variable, viscoplastic model available within Abaqus. We also use different contact conditions with varying pressure sensitivity for heat transfer. The simulations demonstrate that constitutive model selection has a strong effect on the final predicted properties of the forging.*

*Keywords: Forging, Viscoplastic, Anand, Forming, Hot-Working*

## 1. Introduction

Hot forging of engineering alloys poses a complicated, multiphysics problem that couples heat transfer, contact mechanics, rate-and-temperature-dependent material behavior, and the kinetics of microstructural evolution. Resolving this problem experimentally is difficult given the process's highly nonlinear coupling. Simulation is similarly difficult, but still provides the opportunity for improvement given potential insight into the interacting physical processes.

We have selected the forging of a turbine disk preform as an example problem. Turbine disks are typically superalloys that are hot forged into a near net shape. Hot forging accomplishes several objectives in the manufacture of turbine disks. Certainly, given the high strength and deformation resistance, elevated temperatures allow the forming of a near net shape in fewer processing steps. The alloys' high strength also prohibits lower temperature deformation, where large deformations cause cracking of the workpiece and potentially the forging dies. Finally, hot forging with large deformations induce the accumulation of dislocation networks that initiate recrystallization and microstructures that are desired for both strength and creep resistance.

Multiple field variables therefore need to be monitored during simulation. Mises stress indicates the deformation fields and the uniformity of the forging process. Temperature tracks recrystallization, indicates areas of deformation localization, and indicates where die temperatures may exceed acceptable die metal limits. Principal stresses indicate regions of potential cracking and zones of large hydrostatic stress that limit deformation. Plastic strains can serve as a surrogate for deformation localization and indicate both where deformation-induced microstructures encourage recrystallization and how uniform that recrystallization will ultimately be.

## 2. Simulation Details

The forging simulation we have used as an example is provided in Figure 1 below. The actual forging and simulation is axisymmetric, although it is illustrated below in three dimensions to highlight workpiece/die geometry. We selected two native metal constitutive models available within Abaqus 6.14: a simple rate-independent, bilinear elastic-plastic constitutive model with linear hardening, and a rate-and-temperature-dependent model based on the Anand viscoplastic constitutive model (Brown, 1989) which became available with version 6.14. Material constants for the viscoplastic model were selected from the same reference, and the rate-independent model used values in the mid range of flow resistance from the Anand model for the workpiece temperature used in the model.

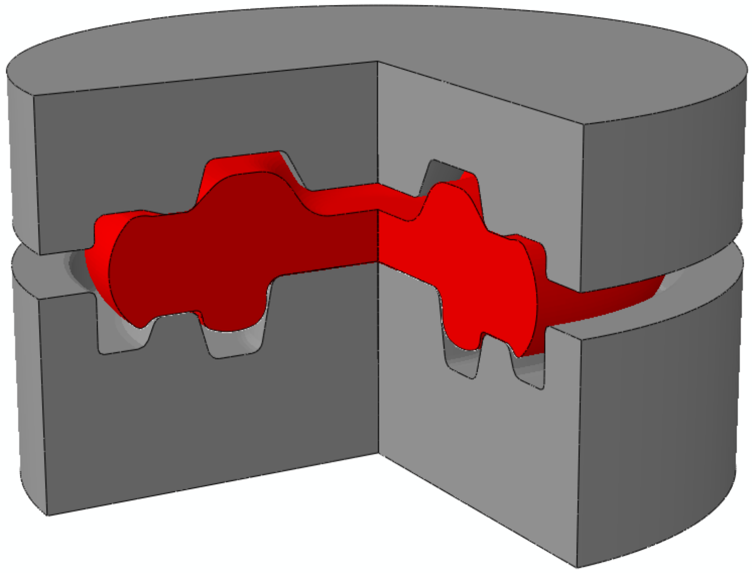

**Figure 1: Geometry of forging process**

The Anand model incorporates an internal state variable that allows the evolution of deformation resistance with time and temperature. The model includes a rate-equation and a scalar, state variable evolution equation, both of which are provided below.

$$\dot{\epsilon}_p = A\, exp\left(\frac{-Q}{R\theta}\right)\left[sinh\left(\xi\,\frac{\tilde{\sigma}}{s}\right)\right]^{1/m} \qquad (1)$$

Here, $\dot{\epsilon}_p$ is the equivalent plastic strain rate, $\tilde{\sigma}$ is the Mises stress, s is the internal state variable, and R is the Gas Constant (8.314 x $10^{-3}$ kJ/mole-K). The evolution equation for *s*, the state variable is:

$$\dot{s} = \left\{h_0\left(1-\frac{s}{s^*}\right)^a sign\left(1-\frac{s}{s^*}\right)\right\}\dot{\epsilon}_p \qquad (2)$$

Here, $s^*$ represents a strain-rate-and-temperature-dependent saturation value of *s*.

$$s^* = \tilde{s}\left[\frac{\dot{\epsilon}_p}{A}exp\left(\frac{Q}{R\theta}\right)\right]^n \qquad (3)$$

Material properties used for the analysis are provided in Tables 1 and 2 below.

**Table 1: Rate-independent Elastic-Plastic Material Properties.**

| Property | Value |
|---|---|
| Elastic Modulus | 201 GPa |
| Yield Stress | 50 MPa |
| Linear Hardening constant | 25 MPa |

**Table 2: Anand Model Material Constants.**

| Property | Value |
|---|---|
| Elastic Modulus | 201 GPa |
| $A$ | $6.346 \times 10^{11}$ sec$^{-1}$ |
| $Q$ | 312.35 kJ/mole |
| $\xi$ | 3.25 |
| $m$ | 0.1956 |
| $h_0 = A_0$ | 3093.1 MPa |
| $a$ | 1.5 |
| $\hat{s}$ | 125.1 MPa |
| $n$ | 0.06869 |
| $S_1$ | 66.1 MPa |
| $A_1, A_2, A_3, A_4, S_2, S_3$ | 0 |

Determining the material constants associated with the Anand viscoplastic model is not trivial. Testing needs to be performed at different strain rates and temperatures, ideally with some experiments that rapidly change strain rate to isolate inherent rate-dependent flow of the alloy from the evolution of the internal state. An example of such a strain rate is illustrated in Figure 2 below.

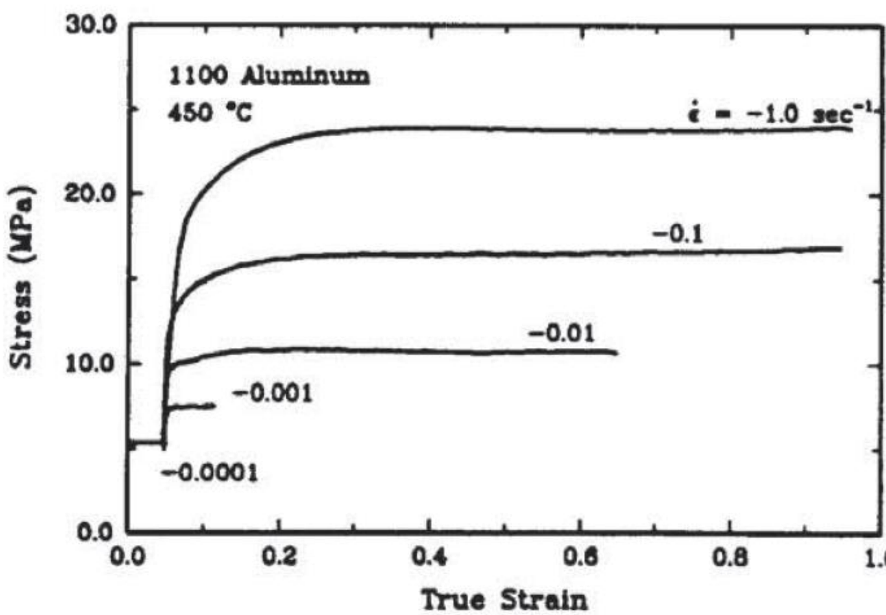


**Figure 2: Strain rate jump test on 1100 Aluminum to evaluate constant-state rate-dependence (Brown, 1989)**

Brown (1989) provides a procedure to extract the relevant constants for both a silicon-iron and an aluminum alloy. Testing should be performed over the range of temperatures and deformation rates anticipated in the forging process. Neither of these alloys undergo either phase changes or dynamic recrystallization under the imposed test conditions. As a result, this model may not be applicable to alloys undergoing phase transitions such as ferrite-to-austenite, or extensive dynamic recrystallization over the temperature or strain-rates of interest. For illustration in this analysis, viscoplastic properties for 3% Si-Fe were used.

In this analysis, the temperature of the workpiece is taken to be 850 Celsius, and the temperature of the dies are assumed a uniform 100 Celsius. Thermally coupled axisymmetric elements are used, permitting full thermomechanical simulation. Exact contact is enforced using Langrange multipliers with a thermal gap resistance of $10^{-5}$ $m^2$-K/W and a coefficient of friction of 0.2. The dies are closed with a velocity of 0.033 meters per second.

Figure 3 provides a comparison of representative mesh deformation before and after forging. Figure 4 more significantly indicates the difference in die force as a function of time resulting from the two constitutive model assumptions. The Anand model predicts approximately a 50 percent higher die force during forging. The difference varies substantially with the assumed properties for the rate-independent constitutive model. The implication is that selection of the constitutive model used for forging simulations has a dramatic effect on predicted forces. Of course these workpiece forces also translate to comparable differences in forces and stresses within the forming dies.

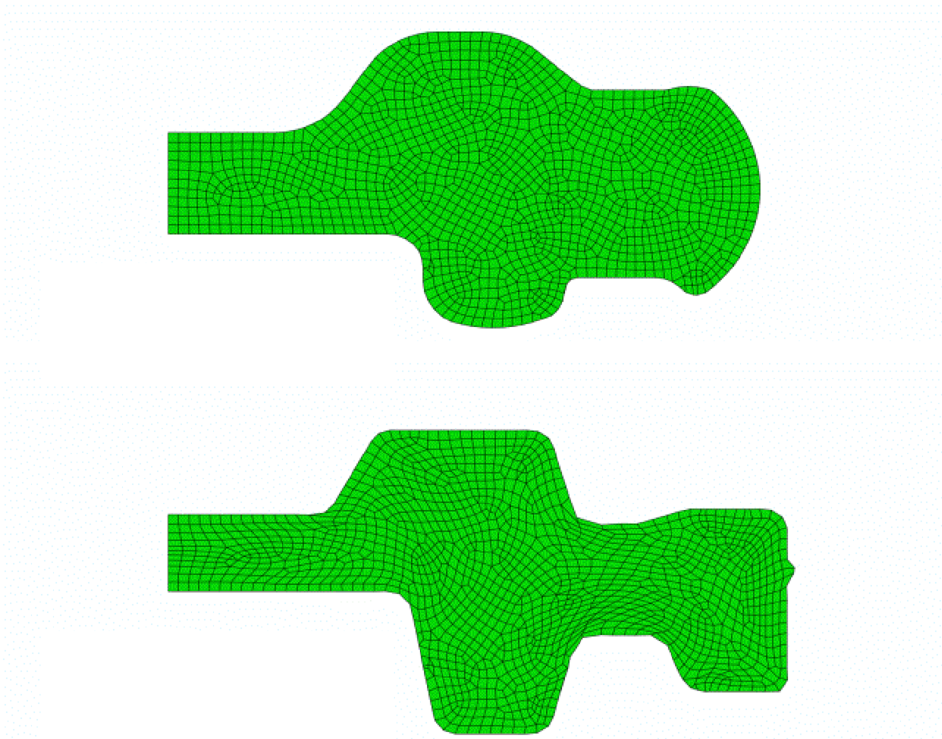

**Figure 3: Change in shape and mesh geometry before and after forging**

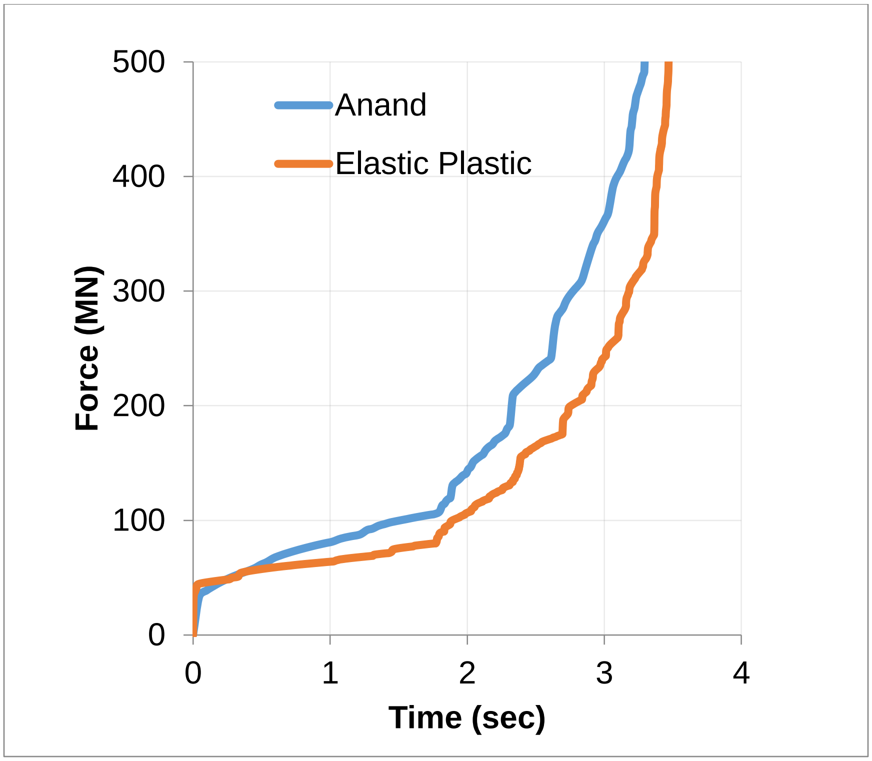


**Figure 4: Variation in die force with time**

Figure 5 provides a comparison of the calculated Mises stress within the workpiece after forging. Once again, there are substantial differences in both stress magnitude and spatial distribution, all resulting from the constitutive model assumption.

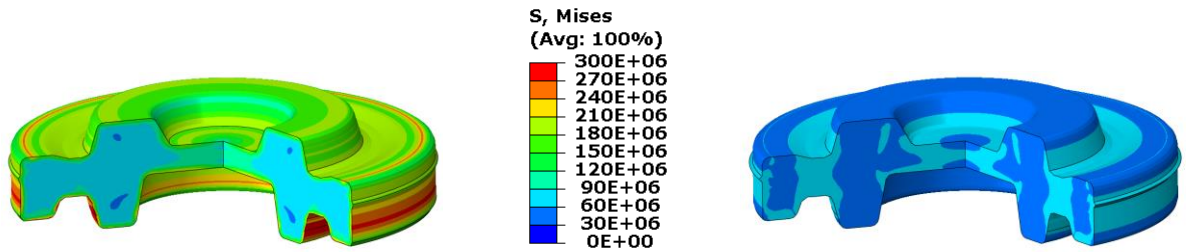


**Figure 5: Von Mises stress state after forging. Rate-dependent Anand model on left, rate-independent simulation on right**

Microstructural evolution is more dependent on strain state than stress state, however. Figure 6 and Figure 7 compare accumulated plastic strain (PEEQ) between the two simulations. A portion of the plastic strain field is magnified on the right side of each figure. Recall that accumulated strain serves as a reasonable surrogate for dislocation density, which subsequently affects the nucleation of recrystallization and any resulting recrystallized grain size.

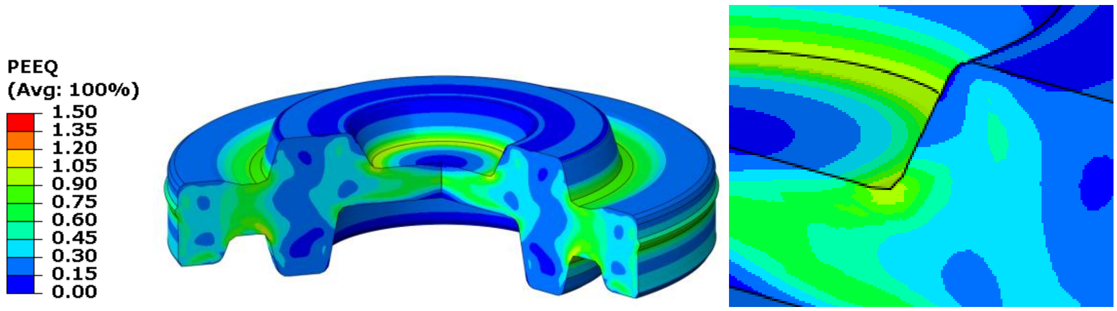


**Figure 6: Anand model simulation results for accumulated plastic strain**

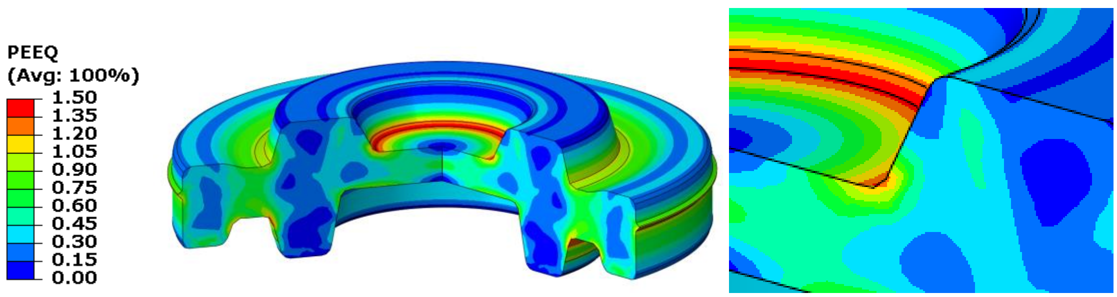


**Figure 7: Rate-independent elastic-plastic model simulation results for accumulated plastic strain**

The two simulations therefore predict different resulting microstructures in different regions of the workpiece. The Anand internal variable model also provides the opportunity to examine the variation in the internal variable *s*, which represents an inherent material state, in this case serving as an alternative measure of dislocation density.

Modeling of recrystallization is difficult (Jang, 2000; Suresh, 2014, Duffett, 2015). Adding this process is beyond the scope of this article, as the recrystallization can be homogeneous or heterogeneous, including processes where dynamic recrystallization occurs through the passage of a recrystallization front through the metal. However, it is important to recognize that simulating hot forging and examining the proper field variables provides insight into whether the deformation field permits or excludes recrystallization. There is furthermore the ability to predict whether recrystallization will proceed to completion, as it is undesirable to arrest the process part way.

## 3. References


1. Brown, S., Kim, K., and Anand, L., "A Internal Variable Constitutive Model for Hot Working of Metals," International Journal of Plasticity, Vol. 5, 1989
2. Duffet, G., "Tutorials for the Simulation of Forging Processes," NAFEMS, 2015
3. Jang, Y-S., Ko, D-C., and Kim, B-M., Journal of Materials Processing Technology, Vol. 101, 2000.
4. Suresh, K, Rao, K., Prasad, Y., Hort, N., and Kainer, K., "Study of hot forging behavior of as-cast- Mg-3Al-1Zn-2Ca alloy towards optimization of its hot workability", Materials and Design, Vol 57, 2014.
5. Abaqus Users Manual, Version 6.14-4, Dassault Systémes Simulia Corp., Providence, RI, 2014